Bulletin of Pure and Applied Sciences.
Geology (Geological Science), Vol.42F, No.1,
January-June 2023: P.88-105
Original Article

Print version ISSN 0970 4639
Online version ISSN 2320 3234
DOI: 10.48165/bpas.2023.42F.1.8
Available online at www.bpasjournals.com

Comparison between SVD-Based and Automatic Geophysical Inversion for Schlumberger VES Data: A Case Study from Konkan Coast, Maharashtra

[1]G. Gupta*, [2]S. Ramachandran and [3]K. Tahama

Author's Affiliations:
[1]KSK Geomagnetic Research Laboratory, IIG, Prayagraj, Uttar Pradesh 221505, India
[2]Dept. of Marine Geology & Geophysics, Cochin Univ. of Science & Tech., Kochi, Kerala 682016, India
[3]Indian Institute of Geomagnetism, New Panvel, Navi Mumbai, Maharashtra 410218, India

***Corresponding Author: G. Gupta,** KSK Geomagnetic Research Laboratory, IIG, Prayagraj, Uttar Pradesh 221505, India
E-mail: gupta_gautam1966@yahoo.co.in

(Received on 25.01.2023, Revised on 20.03.2023, Approved on 12.05.2023, Accepted on 19.05.2023, Published on 15.06.2023)

How to cite this article: Gupta G., Ramachandran S. and Tahama K. (2023). Comparison between SVD-Based and Automatic Geophysical Inversion for Schlumberger VES Data: A Case Study from Konkan Coast, Maharashtra. *Bulletin of Pure and Applied Sciences- Geology,* 42F(1), 88-105.

Abstract:
A comparison is made between the resistivity modeling results obtained from Singular value decomposition (SVD) based geophysical inversion method and a semi-automated inversion scheme to assess the robustness of the SVD method. A total of 30 vertical electrical soundings (VES) data were collected from the hard-rock area of Konkan coastal Maharashtra and modeled using the new method. The results are interpreted so as to identify the coastal aquifers contaminated with saline water in the study area. The SVD- based inversion results suggest a very high resistivity formation in the north-eastern part of the area, presumably due to the presence of laterites at the top, followed by hard and compact basalts beneath. In the south-eastern part of the study area, a very high resistivity zone is evident, due to the presence of laterites and basalts. A very high conductive zone is revealed in the south-western part near the coast signifying extensive influence of saline water ingress, which diminishes from south-west to north-eastern part of the region. It is also seen that the results obtained from the SVD-based algorithm is superior to the conventional inversion scheme.

Keywords: *Singular value decomposition (SVD), resistivity, saline water ingress, Konkan, Maharashtra*

1. INTRODUCTION

Groundwater comprises of major portion of freshwater not tied up as ice and snow in polar ice sheets, glaciers, and snowfields. Groundwater is imperative in supplying water to streams and wetlands, and in providing water for drinking, irrigation, manufacturing, and other uses. The contamination of groundwater by seawater takes place when saline water displaces or mixes with freshwater (Song et al. 2007). Consequently, the layered structures in and around the region have influenced the near surface distribution pattern of electrical properties. Hence modeling and interpretation of direct current (DC) resistivity sounding in such region assume a special implication to understand the inhomogeneous infiltrations of fluids through pores and geologically weak zones, such as faults and fractures, fluid percolation pattern near the subsurface area and the seawater intrusion. To analyze the variation

of groundwater level and its quality due to seawater intrusion and tidal variation, periodic measurement of groundwater level and analysis of quality are necessary, which require installation of observational wells, which would be difficult without knowing the extent of seawater intrusion a priori. Thus, surface geophysical methods such as electrical resistivity or electromagnetic induction could be best alternative for this purpose. Direct current (DC) resistivity sounding method, in which current is introduced directly into the ground through a pair of current electrode, is one of the most popular methods that have been extensively applied for solving hydrological, geothermal, environmental and engineering problems (Zohdy 1989; Ekinci and Demirci 2008).

Forward mathematical models are normally used to relate the measured / observed apparent resistivity data to desired model parameters, true resistivity and layer thickness. The forward modeling is the process of predicting the results of measurements on the basis of some general principles or model and specific conditions relevant to the problem at hand. However, inferring the true resistivity distribution from the apparent resistivity data does not provide precise information due to inherent non-linearity in the data structures (Maiti et al. 2012).

The relation between the observed apparent resistivity and model parameter viz. true resistivity and layer thickness is non-linear in nature. Therefore the estimation of true resistivity distribution versus depth from apparent resistivity data directs to solve the inverse problem. Inverse modeling in contrast starts with data and general principle or model, estimates model parameters by minimizing the error / misfit function set up between the data and model parameter (Menke 1984). Several attempts have been made to solve the inverse problems (Ghosh 1971; Zohdy 1989; Macias et al. 2000; El-Qady and Ushijima 2001; Ekinci and Demirci 2008).

However, these approaches have certain drawbacks as these algorithms rely on the initial parameter chosen for it. The general class "Monte Carlo" e.g., genetic algorithm, stimulated annealing is proven to be useful whilst a good starting model is not available (Rubinstein 1981; Kirkpatrik et al. 1983; Horne and MacBeth 1994; Maiti et al. 2012) for offering global solution. However these methods are computationally expensive. Sometimes it is imperative to search for more robust, cost effective approach for solving non-linear resistivity inverse problem.

The present study area covers the southern part of coastal Sindhudurg district in Maharashtra. Singular value decomposition (SVD) based inversion scheme is used here for estimating true resistivity and layer thickness accurately from Schlumberger apparent resistivity data collected in the study area. A SVD-based scheme is introduced for solving non-linear inverse problem which brought out precise distribution of true resistivity which is of importance, especially the issues related to groundwater exploration in Konkan region of Maharashtra.

1.1 Geological Setting of the Study Area

Evolution of Western Ghats has played a significant role in the genesis of Konkan region (Tandale 1993). The tectonic uplift initiated by the collision of Indian and Eurasian plate during early Tertiary has resulted in the formation of Western Ghats escarpment. The western extension of uplifted Cenozoic plateau that was submerged under waters of Arabian Sea has evolved as Konkan. This narrow coastal belt is arranged in step like terraces, pointing to the recent oscillations in the sea level and submerges as evident from the drowned valleys, lagoons and sand bars; wave cut cliffs and platforms are also common along the coast line indicating changes in the sea level.

The basaltic flows and intrusive, intertrappean and laterite cappings are common geological features of Maharashtra coast (Tandale 1993). A greater part of the coastal belt of Maharashtra is developed as a result of several morpho-dynamic cycles. The basement of basalt flows was formed by extruded Deccan volcanic activity during late cretaceous-early tertiary period with a minor metamorphosed Dharwars in the southern most section of Sindhudurg. The Precambrian granites and gneiss quartzites and

amphibolites are exposed in the Vengurla region that continues up to the Karwar (Karnataka State). A wide range of landforms developed due to fluvial and marine activity during the tertiary and quaternary periods is displayed in the coastal region.

The volcanic flows in Deccan Trap region are almost horizontal throughout the region. There are many lava flows with varying thickness from 10 to 160 m. Variation in thickness of the trap flows is attributed by mainly to pre-Trap topography. These massive compact lava sequence have low permeability, there is significant migration of water through faults, fractures columnar jointing and vesicles (Morgan 1972). A general regional strike is in variation from NS to NNW. Several lineaments have been delineated in the Deccan Trap region. Structural shear zones are speculated to exist along the lineament, based on study of imageries and some field observations (Tandale 1993). Though Sindhudurg district has no earlier history of earthquake, still it comes under zone III. The proximity of Western Ghats fault scarp and evidence of neo-tectonic activities in the Konkan area point to the earth movements in recent past and possibility of an earthquake cannot be ruled out. It is also evident that this region is cris-crossed by several lineaments and faults. It thus assumes importance for any neo-tectonic activity.

The present resistivity survey area covers the major parts of Vengurla-Sawantwadi in Konkan region (Latitude 15.75$^{\circ}N$to Latitude15.90$^{\circ}N$) to (Longitude 73.62$^{\circ}E$ to73.87$^{\circ}E$) (Figure 1). The measurements were taken using the SSR-MP-AT instrument (manufactured by IGIS, Hyderabad) with a maximum current electrode separation (AB) as 200 m. In order to improve the quality of the data, the resistivity meter performed a stack of minimum three for each data point. The existing geophysical and geological studies show that the shallow distribution of the resistivity is important for understanding the fractures, voids, conduits, faults and lineament pattern of the area. The exposed basement is fractured at many places of the area which could be speculated as shear zones. In view of the established utility of resistivity method in locating and demarcating the fractured and weathered zones, it was worth to conduct electrical resistivity over the area to get a precise true resistivity value against depth via very powerful algorithm which in turn would throw light into the insight of management of groundwater resources.

Archean Dharwars, Kaladgi formation (Precambrian), Deccan Trap lava (Upper Cretaceous to lower Eocene age), laterite (Pleistocene) and Alluvial deposits (Recent to sub-recent) are the water-bearing formations seen in Sindhudurg district (Sarkar and Soman 1986). The Kaladgi formation does not form potential aquifer in the district as it occurs in very limited patches. The alluviums too have limited areal extent found mainly along the coast (CGWB 2009).

In Dharwarian metasediments the unconfined aquifer is developed down to depth of 15 m below ground level (bgl) (CGWB 2009). The unconfined aquifer in the Kaladgi rocks is developed down to depth 10-12 m bgl. In the basaltic terrain, groundwater occurs under unconfined conditions in the phreatic zone up to a depth of 15 m in the weathered zone, fractures and joints in the massive and weathered /fractured vesicular basalt (CGWB 2009). The unconfined aquifer in the Deccan Traps is developed due to weathering and jointing of upper flow in basalt down to depth of 15-20 m bgl. Laterite has better porosity due to intricate network of sinuous conduits, joints and fractures. The local water table aquifer develops in the top most layer down to depth of 20 m bgl under unconfined conditions (CGWB 2009). The groundwater in the alluvium occurs in inter-granular pore spaces of sands, gravel and silts (CGWB 2009) at relatively shallow depths of 2-10 m bgl.

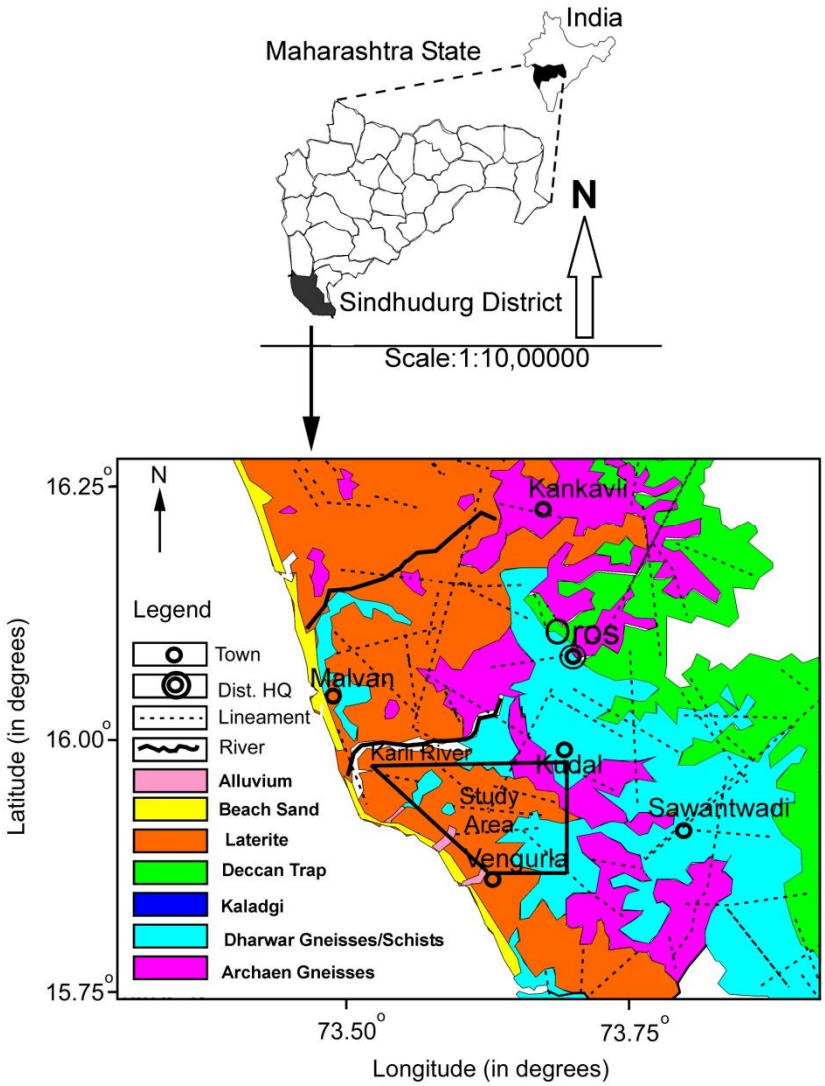

Figure 1: Geological map of Sindhudurg district, Maharashtra, India. Also shown is the study area.

1.2 Occurrence and Character of Groundwater in Study Area

The infiltrated rainwater enters in to the subsurface and stored in the porous but impermeable space in the rock formation. The infiltration of groundwater depends upon quantity of rain, soil characters (both physical and chemical) and the concentration of porous space and packing of the rock type, fracture present in the rock type etc (Puranik 2009). It is noteworthy that opening/ porous space in rocks mean the space between the particle in case of unconsolidated and semi unconsolidated rocks, whereas for consolidated (hard rock) the porous opening means the fractures, joints, shear zones and fault planes. Such 'opening' in hard lateritic/basaltic rock in the area occurs due to structural/orogenic activities, thus creating the secondary porosity/opening which is developed after the formation of rocks (Puranik 2009). The groundwater normally occurs under phreatic (below the water table)/unconfined conditions. The 'openings' are available in a network in the area which serves as conduits thus helping groundwater to flow and store. In the highly fractured (not weathered rock) rocks the type of porosity is fracture porosity (Verma et al. 1980). In these

fracture rocks groundwater moves both vertically and horizontally depending upon the opening bounded by clay.

2. MATERIALS AND METHODS

2.1 Forward modeling

Schlumberger sounding is a well-accepted method used in DC Resistivity survey. In this technique, the correlation between the apparent resistivity (ρ_a) and the layer parameters (layer thickness and layer true resistivity) can be expressed by the integral equation given by Koefoed (1970), considering an earth model consisting of homogeneous and isotropic layers as,

$$\rho_a(s)=s^2 \int_0^\infty T(\lambda) J_1 \lambda(s) d\lambda \quad (1)$$

Where, s is the half the current electrode spacing (AB/2) in Schlumberger electrode configuration, J_1 denotes first- order Bessel function of the first kind and λ denotes the integral variable (equal to $1/(\frac{AB}{2})$) and $T(\lambda)$ is the resistivity transform function. The recurrence relationship of the resistivity transforms function ,$T(\lambda)$ after Koefoed (1970) is given as,

$$T_i(\lambda) = \frac{T_{i+1}(\lambda)+\rho_i \tanh(\lambda h_i)}{[1+T_{i+1}(\lambda)\tanh(\lambda h_i)/\rho_i]} \quad (2)$$

i= n-1, …..1

Where, n denotes the number of layers, $\rho_i$and h_i are the true resistivity and thickness of the i^{th} layer respectively.

2.2 Inversion scheme

Geophysical inversion is a tool for recovering information on subsurface physical properties acquired from geophysical field data. Geophysical inversion aids in elucidating complex data sets by removing topographic effect and provides a quantitative model that can be analyzed. The non-linear least-squares inversion method is based on the approximation of the model by a linear one and to refine the parameters by successive iterations. The forward model is based on the explicit relation between physical models to the observed field data. However, inversion of geoelectrical data is an ill-posed problem because the contradictory information on model parameter cannot be assessed due to lack of information. Therefore minute changes in the field data may lead to drastic changes in the model. Choosing the correct initial model is thus important for an effective output model. As advocated by Roy (1999), this problem can be addressed by introducing damping into the system of equations.

This resulted in a solution of damped least squares which can be written following (Menke 1984) as,

$$\Delta m = (G^T G + \beta^2 I)^{-1} G^T \Delta d \quad (3)$$

Where, Δm is the parameter correction vector; Δd is the data difference vector or discrepancy vector, G is the Jacobian matrix containing partial derivatives of data with respect to the initial model parameters. I is the identity matrix, and β is the damping factor which is a scalar quantity controlling both speed of convergence and solution. This solution is also known as Tikhonov regularization (Levenberg 1944; Marquardt 1963; Menke 1984).

2.3 Singular value decomposition (SVD)

Singular Value Decomposition (SVD) is a widely used technique in several domains of geophysical inversion for decomposing a matrix into several component matrices, exposing many of the useful and interesting properties of the original matrix. SVD has numerous applications in statistics, machine learning computer science, astronomy and eigen decomposition including compressing, de-noising, and data reduction. It reduces a matrix to its constituent parts in order to make certain subsequent matrix calculations simpler.

An $n \times norn \times m$ matrix G is factorized in equation (3) as follows,

$$G = UQL^T \quad (4)$$

Where for n data and m parameters, U($n \times m$) and $L(m \times m)$ are two orthogonal matrix, containing respectively the data space and the parameter space eigen vectors and Q is a (m×m) diagonal matrix containing at most r non-zero

eigen values, with a condition $r \leq m$. Here the Jacobian matrix is introduced to increase the stability of solving the inverse problem. Following this, the weighting matrix is dropped which cause no loss of generality. When the $G^T G$ becomes singular (det$G^T G$ = 0) no solution is obtained. If $G^T G$ is almost singular (det$G^T G$<<1) large parameter variation is observed. These diagonal entities in matrix Q($\propto_1, \propto_2, \ldots\ldots, \propto_p$) are called singular values of G. The above equation is not defined if one of the singular values equals zero. Therefore, damping factor β is introduced for stabilization. The SVD-based damped least squares solution is written as,

$$\Delta m = (LQ^2L^T + \beta^2 I)^{-1} LQU^T \Delta d \quad (5)$$

We get the form by adding the damping factor to the diagonal elements

$$(LQ^2L^T + \beta^2 I)^{-1} = \{L\text{diag}(\propto_j^2)L^T + \beta^2 I\} = L\text{diag}(\propto_j^2 + \beta^2)\, L^T \quad (6)$$

We write the inverse of the equation (4) as follows,

$$(L\text{diag}\{\propto_j^2 + \beta^2\}L^T)^{-1} = Ldiag\{\tfrac{1}{\propto_j^2+\beta^2}\}L^T \quad (7)$$

Substituting the equation (5) in equation (3) we obtain,

$$\Delta m = Ldiag\{\tfrac{1}{\propto_j^2+\beta^2}\}L^T LQU^T \Delta d \quad (8)$$

We obtain the parameter correction vector as:

$$Ldiag\{\tfrac{1}{\propto_j^2+\beta^2}\}U^T \Delta d \quad (9)$$

Equation (8) provides damped least-squares solution through the SVD. The damping factor is set at a large positive value in the initial model and subsequently, at every iteration, the damping factor is multiplied by a factor less than unity so that the least-squares method dominates near the solution. In addition to the information related to model parameter resolution and covariance analysis, SVD provides numerically stable results (Meju 1994). It is the most known and widely used matrix decomposition method. All matrices have an SVD, which makes it more stable than other methods, such as that the least-squares methods dominate near the solution (Meju 1994). The damping factor is calculated after Arnason and Hersir (1988) as,

$$\beta = \alpha_w \Delta c^{1/w} \quad (10)$$

Where w is the test number for the damping factor at any iteration, α is the parameter eigen value and the term Δc is given by,

$$\Delta c_r = \frac{c_{r-1} - c_r}{c_{r-1}} \quad (11)$$

Where $c_{r-1}$the misfit value is obtained at previous iteration and c_r is the misfit found at the current iteration. In this study, equations (9) and (10) were used to set the damping factor at each iteration.

2.4 Interactive inversion scheme (IPI2WIN)

IPI2WIN is designed for interactive semi-automated interpretation of vertical electrical sounding data, magnetotelluric data and induced polarization data (Bobachev 2003). Targeting at the geological result is the specific feature distinguishing IPI2WIN among other popular program of automatic inversion. Due to handy control the interpreter is able to choose from a set of equivalent solutions the best one fitting the both geophysical data and geological data. This approach provides the opportunity to use a priori geological data and extract information to the greatest possible extent in the complicated geological situations. For viewing curves and models, the pseudo cross-section of a specified value and resistivity cross-section are displayed (VES-IP mode), which can be used for interpretation.

2.5 MATLAB algorithm and implementation

The proposed scheme is implemented in MATLAB environment. The flowchart of the total inversion scheme is given in figure 2. The VES data is checked manually and the necessary manual correction is done first. Then the apparent resistivity data is prepared in chart against different AB/2 spacing. For the inversion process, the initial model is chosen based on the *a priori* geological/geophysical knowledge of the survey area. Based on the

initial model parameter (true resistivity and true layer thickness) the forward modeling calculation is done using the forward modeling equations. Then the theoretical data predicted by forward modeling is compared with the observed apparent resistivity data.

2.6 Program Description

The main program reads the observed apparent resistivity data and the AB/2 spacing from the data file and inverts apparent resistivity data by using damped least- squares solution with SVD. The program also uses the basic plotting commands for the graphic of the inversion results.

The misfit error/Root Mean Square error (RMSE) is calculated between the observed data and the theoretical predicted data. RMS error is defined as the square root of mean of difference of observed and calculated values. If the error is less than the permissible/tolerance limit, the program is stopped otherwise the model parameters are changed and the forward calculation and comparison are followed as per the flowchart (Figure 2). The program may also stop if it meets other criteria such as reaching the maximum iteration etc. In the present case, the maximum iteration has been chosen to be 500.

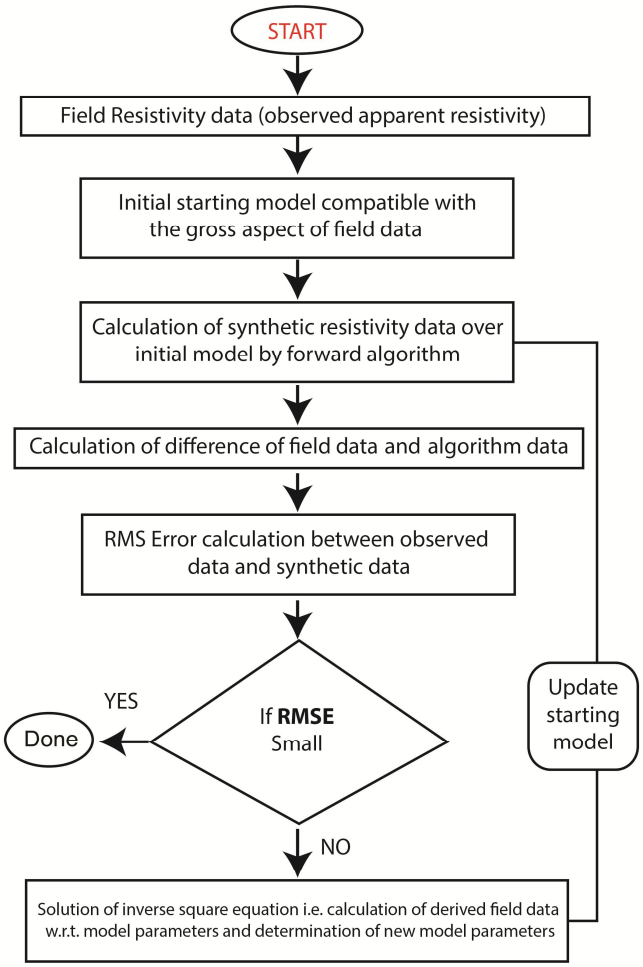

Figure 2: The flowchart of the total inversion scheme.

However, the program inverts all the data sets before the maximum assigned maximum iteration number. The trial and error is the standard process for choosing the value suitable damping parameter constant. The algorithm is fast and usually provides stable solution. The algorithm takes few seconds for inversion of individuals sounding curves. The Jacobian function computes the partial derivatives of parameters numerically by using a user-selected difference interval value and forms the Jacobian matrix. The function VES1Dmod calculates the apparent resistivity data from the given values for Schlumberger electrode configuration by using the filter coefficients (Nyman and Landisman 1977).

2.7 Interpretation Techniques

The concept of apparent resistivity is the key to the interpretation of resistivity field data. While the interpretation of profiling data is often qualitative, the quantitative interpretation is the sounding field data of each sounding point. The curve matching technique was successfully used till Koefoed (1970) revolutionized the computation of resistivity master curves by the application of linear digital filter after which computer aided interpretation and inversion techniques came more into picture. In the interpretation of resistivity sounding data, the geological formations are assumed to be horizontal or nearly horizontal. The ground could have two, three or multi layers with different resistivity and thickness. In sedimentary basin there are layers of sandstone, shale, limestone etc., whereas in hard rock terrains, soil and weathered rock formations overlie fresh rock approximating a three- layer section. If top soil lies directly over the fresh rock, there are dominantly two layers.

2.8 One dimensional modeling

The linearization of inverse resistivity problems and minimization in a least-squares manner was suggested by Inman (1975) to find the best possible solution. Information such as noise level (random error) associated with data, and the eigen values and eigen vectors of the system matrix which are essential to study model parameter resolution are also discussed therein. It can be shown that linear estimation from non-orthogonal data (i.e. nearly singular data) could be refined or improved by using biased estimators; this technique has been termed ridge regression (Inman 1975).

Marquardt (1963) established the similarities between the generalized inverse method and ridge regression methods for problems with small eigen values. Since most common resistivity problems involve small eigen values, the ridge regression for inversion of resistivity data was introduced by Inman (1975). Parker (1994) addressed the non-uniqueness of 1-D inverse resistivity problems using a bi-layer expansion method. His models consisted of layers having uniform thickness, and solution determined the optimum number of layers and layer thickness that would minimize the deviation in a least-squares manner.

The basic limitation of all 1-D resistivity inversion methods is that they only consider vertical variations in the earth's resistivity: thus they are generally limited to cases with simple, planar spatial variations, and cannot be applied to evolving situations such as a rise in situ monitoring or strongly to three-dimensional structures.

3. RESULTS AND DISCUSSION

3.1 Comparision between IPI2WIN software and the SVD based inversion code

The DC resistivity sounding with Schlumberger array was carried out at 30 VES stations using electrode spacing starting from AB=2 up to m in successive steps (Figure 3). The field sites were chosen on the basis of accessibility in order to attain the objective. These 30 DC resistivity sounding data is inverted using SVD based inversion scheme and IPI2WIN software. The one dimensional inversion results are shown in the Figures 4-6. The figures show the SVD-based inverse resistivity results on left side, and the image on the right side represents the inversion using IPI2WIN software.

A comparison of resistivity values of layers and thickness obtained using the IPI2WIN Software as well as the geophysical inversion code is given in Table 1. The comparison of RMS error (RMSE) of results using SVD-based inversion code and IPI2WIN software is listed in Table 2. It is observed that the RMS error is the least when inversion is done with the SVD-based geophysical inversion code.

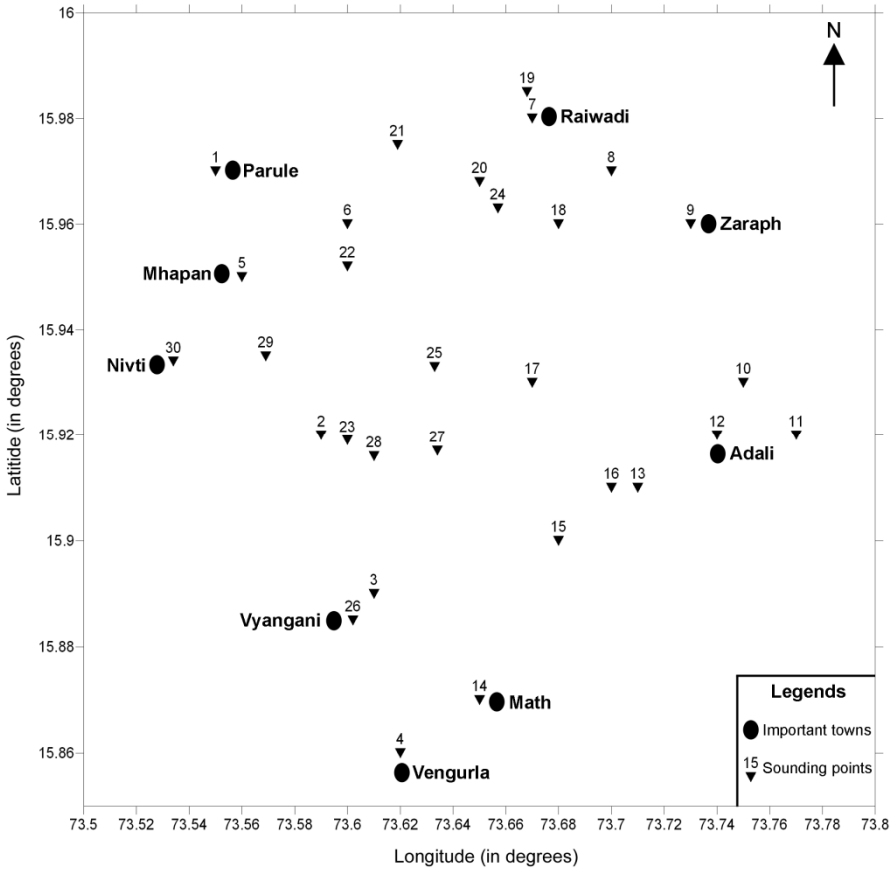

Figure 3: Location map of VES stations in Sindhudurg district of Maharashtra.

Table 1: Comparison of resistivity values of layers and thickness obtained using IPI2WIN Software and the geophysical inversion code

VES No.	Using inversion code			Using IPI2WIN software		
	ρ values	Thickness (m)	Depth (m)	ρ values	Thickness (m)	Depth (m)
1	161	0.592	0.592	168	0.568	0.568
	49.9	2.26	2.852	58	1.95	2.52
	501.2	55.4	58.25	503	55.3	57.8
	34354	--	--	34382	--	--
2	2112.1	0.435	0.435	2187	0.421	0.421
	1515	6.705	7.14	1544	6.58	7.01
	409	29.6	36.8	417	29.1	36.1
	0.99	--	--	1.03	--	--
3	2598	3.57	3.57	2670	3.48	3.48
	311	21.8	25.42	330	20.6	24.1
	74102	--	--	75690	--	--
4	2054	2.08	2.08	2252	1.9	1.9
	954	7.73	9.81	998	7.39	9.29
	2537	9.681	19.49	2661	9.23	18.52
	239	--	--	292	--	--
5	508	0.635	0.635	582	0.555	0.555
	302	7.81	8.451	366	6.45	7
	929	--	--	1019	--	--
6	708	0.643	0.643	731	0.623	0.623
	401.2	4.037	4.68	424	3.82	4.443
	312	56.06	60.74	345	50.7	55.143
	17074	--	--	17151	--	--
7	104	1.09	1.09	138	0.826	0.826
	10.5	7.14	8.23	19	3.95	4.776
	45509	--	--	45587	--	--
8	186	0.557	0.557	201	0.516	0.516
	18	2.94	3.5	25	2.12	2.63
	622	26.3	29.8	646	25.4	28.1
	45438	--	--	45684	--	--
9	202	0.462	0.462	223	0.419	0.419
	21	11.36	11.826	27.4	8.71	9.13
	38006	--	--	38217	--	--
10	1054	0.472	0.472	1182	0.421	0.421
	212	1.04	1.521	257	0.866	1.29
	96	9.722	11.243	118	7.91	9.2
	3819	--	--	3998	--	--
11	186	0.495	0.495	195	0.473	0.473
	6.54	0.77	1.27	7.81	0.652	1.12
	35204	--	--	35502	--	--
12	2358	0.57	0.57	2550	0.53	0.53
	365	6.315	6.88	403	5.72	6.25
	201	6.39	13.27	232	5.54	11.8
	1486	--	--	1519	--	--
13	205	1.451	1.451	226.3	1.315	1.315

	38	2.18	3.6	42.7	1.944	3.258
	1084	23.34	26.94	1219	20.76	24.02
	142582	--	--	143539	--	--
14	396	0.854	0.854	409	0.8271	0.8271
	1496	6.46	7.315	1507	6.414	7.241
	193	26.3	33.68	202.4	25.15	32.39
	1014	--	--	1082	--	--
15	2361	0.47	0.47	2401	0.463	0.463
	298	6.96	7.43	320	6.49	6.95
	67	6.55	13.98	78.2	5.62	12.6
	1896	--	--	1935	--	--
16	95.6	1.67	1.67	109	1.47	1.47
	29	1.66	3.33	36.1	1.34	2.81
	32388	7.72	11.05	32506	7.7	10.5
	124.6	--	--	166	--	--
17	1702	1.3	1.3	1765	1.26	1.26
	988	4.36	5.66	1015	4.25	4.25
	212	7.71	13.37	274	5.97	10.22
	51	15.44	28.8	63	12.5	22.72
	3059	--	--	3103	--	--
18	610	0.93	0.93	639	0.893	0.89
	199	0.89	1.82	242	0.733	1.63
	673	1.89	3.71	719	1.77	3.40
	37.2	8.75	12.46	46.6	6.99	10.39
	1718	--	--	1741	--	--
19	344	0.55	0.55	378	0.508	0.51
	17.6	4.9	5.45	20.4	4.23	4.74
	17228	--	--	17643	--	--
20	3204	0.65	0.65	3574	0.584	0.58
	402	0.654	1.3	439	0.599	1.18
	2458	1.73	3.03	2848	1.5	2.68
	115.9	23.1	26.18	142	18.9	21.58
	2101	--	--	2240	--	--
21	998	0.82	0.82	1078	0.766	0.766
	386	1.09	1.916	419	1.01	1.776
	1210	2.83	4.74	1399	2.45	4.226
	38.2	12.7	17.47	47.7	10.2	14.426
	3398	--	--	3488	--	--
22	204	0.7	1.32	219.5	0.654	0.654
	450.2	1.43	2.75	472.6	1.367	2.021
	946	2.9	5.65	961	2.856	4.877
	104	9.18	14.8	160	5.97	10.847
	32105	12.6	27.4	32458	12.48	23.327
	513.9	--	--	533.8	--	--
23	152.1	0.688	0.688	174.6	0.6	0.6
	466	0.694	1.38	494.7	0.654	1.254
	173.5	26.07	27.4	199.5	22.68	23.934
	104	30.44	57.84	121.4	26.08	50.014
	212.8	--	--	238	--	--
24	3088.6	0.499	0.499	3214	0.48	0.48

	176.5	2.82	3.32	201	2.48	2.96
	1503	2.78	6.1	1586	2.64	5.6
	37.6	9.46	15.5	45	7.91	13.51
	23115	--	--	23513	--	--
25	130	0.97	0.97	148	0.86	0.86
	65.6	0.73	1.7	72.5	0.666	1.526
	1410	4.49	6.19	1515	4.18	5.706
	38.5	7.75	13.94	44.9	6.65	12.356
	677.9	--	--	718	--	--
26	147	1.68	1.68	154	1.61	1.61
	1578.2	5.61	7.29	1613	5.49	7.1
	88	41.06	48.3	92.9	38.9	46
	8701.5	--	--	8761	--	--
27	381.5	0.46	0.46	417	0.425	0.425
	15.6	0.74	1.2	20.2	0.573	0.998
	702	5.59	6.79	726	5.41	6.408
	10.1	14.5	21.29	15.2	9.64	16.048
	12015	--	--	12322	--	--
28	80.3	1.07	1.07	85.4	1.01	1.01
	16.5	9.37	10.44	18.4	8.41	9.42
	30425	--	--	30661	--	--
29	212.8	1.44	1.44	242.5	1.264	1.264
	45.8	0.51	1.95	51.56	0.458	1.722
	92.8	31.04	32.99	103	27.97	29.692
	444.3	--	--	496.4	--	--
30	0.8	1.64	1.64	0.938	1.4	1.4
	0.526	26.81	28.4	0.624	22.6	24
	322	--	--	379	--	--

Table 2: Comparison of RMS Error (%)

VES	Using inversion code	Using IPI2WIN
1	2.03	2.48
2	3.93	7.54
3	2.98	5
4	2.77	6.31
5	1.08	2.58
6	2.32	2.65
7	2.97	16.1
8	2.8	3.71
9	1.04	3.08
10	0.298	2.85
11	1.513	5.41
12	2.7	3.1
13	1.1	1.71
14	0.17	1.21
15	3.01	3.06
16	2.01	2.3
17	2.12	2.54
18	1.54	2.28

19	3.99	10.4
20	3.02	3.47
21	1.67	3
22	0.61	1.01
23	0.64	0.922
24	2.87	2.88
25	0.54	2.85
26	2.27	4.02
27	1.1	10.9
28	3.31	5.08
29	1.27	1.31
30	0.04	3.68

In the Figures 4-6, the open circles indicate the field data and the solid lines (red in colour) indicate the synthetic data. In Table (1) the resistivity values, the thickness of each layers and the depth for each VES data points are given. From the inversion results it is found that there are two-layer, three-layer, four-layer, five-layer and seven-layer cases. The types of VES resistivity sounding curves that occurred the most are H type, HK type, HA type, KH type and HKH type. Most of the three layered cases show H type resistivity sounding curves. HA type curves are observed mostly in four layered case. In all the five layered cases HKH curves are seen.

Section of the curve between 50 to 100 Ω-m are likely to be freshwater, while part of the curve below 20 Ω-m are likely to be brackish water, which is a mixture of fresh water and seawater, that is not suitable for either human consumption or irrigation. Sections with very low resistivity values are expected due to seawater or brine water and both unusable for human consumption and irrigation.

Figure 4a shows the SVD-based inversion results of VES point 1. The curve type suggest an HA - type. Among four layers, the first layer reveals a resistivity value of 161 Ω-m, while the second layer is having a resistivity value of 49.9 Ω-m, indicating the presence of brackish water. The resistivity value thereafter monotonously increases to 34354 Ω-m till the fourth layer, indicating hard basement rock structure at deeper levels.

The inversion results of VES point 2 is shown in Figure 4c. Here the resistivity value decreases from 2112.2 Ω-m to 0.99 Ω-m from first to fourth layer. This suggests the presence of saline water in the fourth layer indicating saltwater intrusion. At sounding point 3 (Figure 4e), a low value of resistivity (311 Ω-m, second layer) is sandwiched between the first (resistivity value 2598 Ω-m) and the third (resistivity value 74102 Ω-m) layers. It is showing an H- type sounding curve.

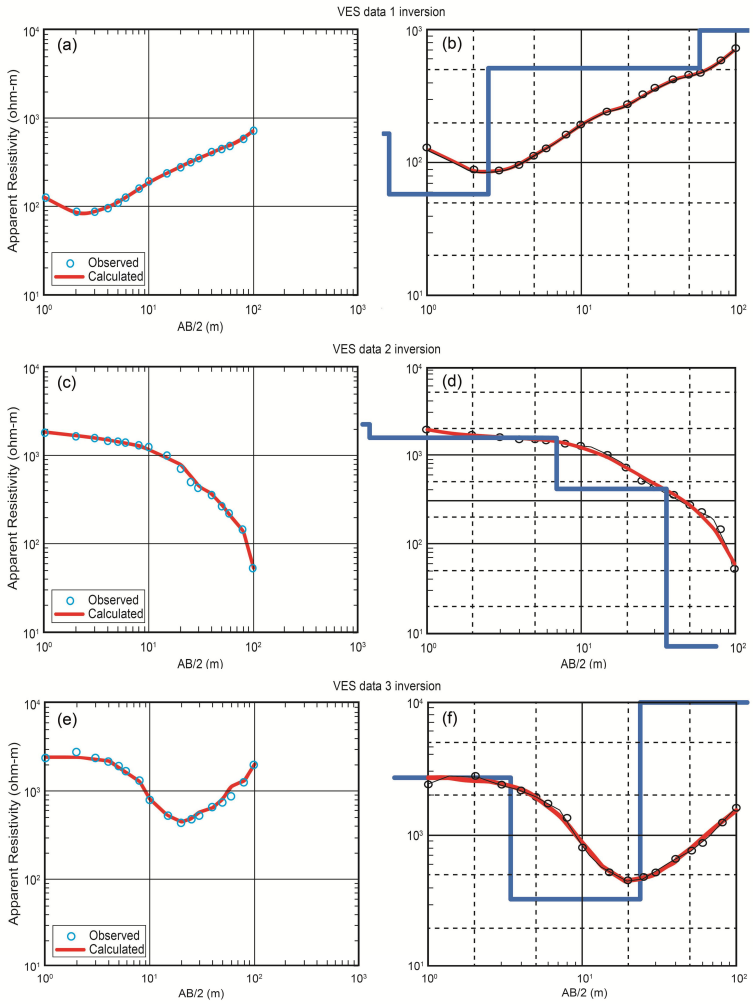

Figure 4 (a, c, e): One dimensional inversion of VES data using SVD-based inversion code; 4 (b, d, f) using IPI2WIN software

At sounding point 7 (Figure 5a), the resistivity value decreases from 104 Ω-m in the first layer to 10.5 Ω-m in the second layer indicating brackish water at a depth of about 8 meters and then increases to 45509 Ω-m indicative of hard basement rock. Similarly at VES point 8 (Figure 5c), the presence of brackish water saturated region at a depth of about 3.5 meter is indicated by lower resistivity value of second layer (18 Ω-m). At VES point 10 (Figure 5e), four layers are identified and a relatively low resistivity value (96 Ω-m) in the third layer indicates that the region is saturated with fresh water.

At VES 11, a low resistive second layer (6.54 Ω-m) indicates the possibility of seawater ingress (Figure 6a). Five layers are revealed at VES point 24 (Figure 6c) with HKH- type resistivity sounding curve. The resistivity value decreases from 3088.6 Ω-m in the first layer to 176.5 Ω-m in the second layer indicating a shallow aquifer at a depth of 3.32 meters. Further, a high resistive (1503 Ω-m) third layer is observed followed by a decrease in resistivity value to 37.6 Ω-m in the fourth layer. This is indicative of fresh water at a depth of about 15.5 meters. The fifth layer suggests high resistivity value (23115 Ω-m) signifying hard rock basement structure. Lower resistivity values obtained at VES sounding point 30 (Figure 6e) indicate the effect of sea water intrusion as the sounding point is close to the West coast, which is due to brine water suggesting high concentration of sodium and chloride.

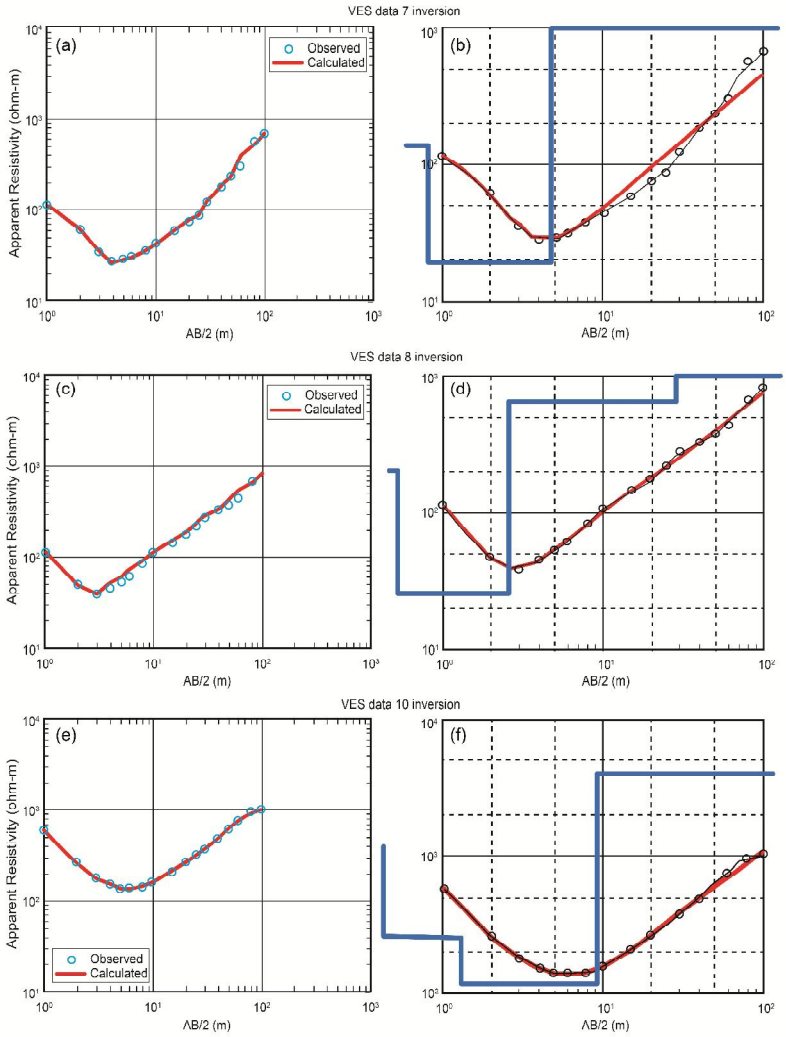

Figure 5 (a, c, e): One dimensional inversion of VES data using SVD-based inversion code; 5 (b, d, f) using IPI2WIN software

Geochemical studies of water sample in this region (Gupta et al. 2014) reported that the EC values recorded at VES 2 and VES 30 falls beyond the acceptable level for drinking as prescribed by World Health Organization (WHO 1984), and were attributed due to intrusion of saline water from Arabian Sea. Also the TDS value at these sites exceeds the acceptable limit prescribed by WHO (1984). The Cl^- concentration recorded at VES 2 and VES 30 falls beyond the permissible limit (200 mg/l). The high concentration of Cl^- at these places is primarily due to the saline water intrusion and secondarily due to the influence of discharged agricultural, industrial and domestic waste waters. Such intrusion phenomena occur owing to the hydraulic connection between groundwater and seawater. Saline water has higher mineral content than freshwater, thus it is denser and has a higher water pressure. As a result, ingress of saltwater beneath the freshwater in inland aquifers is predominant.

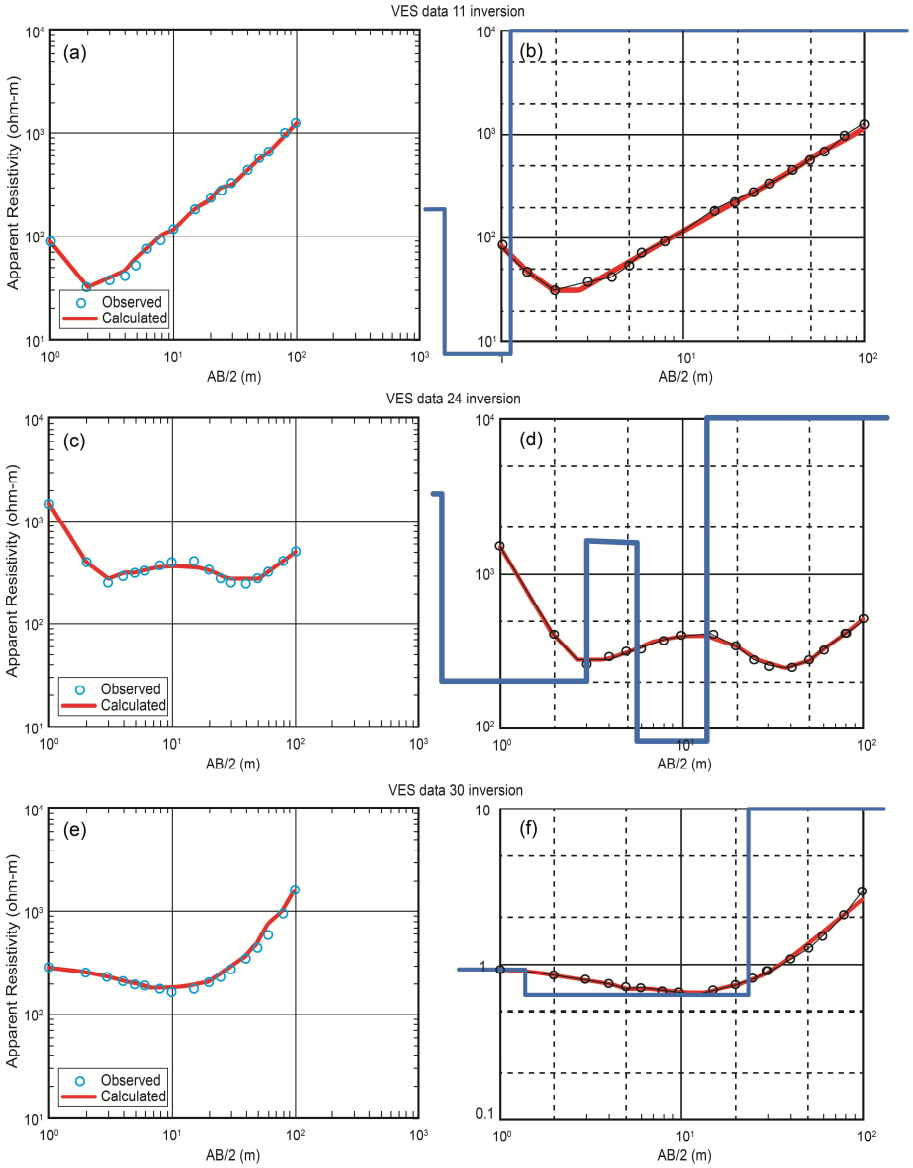

Figure 6 (a, c, e): One dimensional inversion of VES data using SVD-based inversion code; 6 (b, d, f) using IPI2WIN software

4. CONCLUSIONS

The salient results obtained from the present study is as follows,

1. Singular Value Decomposition (SVD) based direct current electrical resistivity inversion scheme is developed and applied to the Schlumberger VES data collected over Konkan coastal region in Maharashtra. The inversion scheme is fast, stable and cost effective.

2. The results obtained using the SVD based geophysical inversion code showed the least value of RMS error when compared with results using IPI2WIN software.

3. The method is tested on synthetic data set and then applied to a 30 DC resistivity data-set acquired from Konkan coast of Maharashtra. Besides providing some new and detailed information, the present results also corroborate well with existing geochemical results.

Thus the method provides potential means for mapping resistivity structure of the coastal area of Maharashtra which will help in studying salt water ingression from the Arabian Sea.

5. ACKNOWLEDGEMENTS

The authors are thankful to the Director, Indian Institute of Geomagnetism, New Panvel for kind permission to publish the work. The authors express their gratitude to Shri B.I. Panchal for drafting the figures.

6. REFERENCES

1. Arnason K., Hersir G.P. (1988). One dimensional inversion of Schlumberger resistivity soundings. Computer program, Description and user's Guide: The United Nations university, Geothermal Training, Report 8, 59.
2. Bobachev C. (2003). IPI2Win: A windows software for an automatic interpretation of resistivity sounding data. Unpubl Thesis, Moscow State University, Moscow, Russia.
3. Central Ground Water Board (CGWB) (2009). Ground water information Sindhudurg district Maharashtra. Technical Report, 1-16.
4. Ekinci Y.L., Demirci A. (2008). A Damped least squares inversion program for the interpretation of Schlumberger sounding curves. *J Appl Sci,* 8(22):4070-4078.
5. El-Qady G, Ushijima K (2001) Inversion of DC resistivity data using artificial neural networks. *Geophys Prospect,* 49, 417–430.
6. Ghosh D. (1971). The application of linear filter theory on the direct interpretation of geoelectrical resistivity sounding measurements. *Geophys Prospect* 19, 192-217.
7. Gupta G., Maiti S., Erram V.C. (2014). Analysis of electrical resistivity data in resolving the saline and fresh water aquifers in west coast Maharashtra, India. *J Geol Soc India*, 84, 555-568.
8. Horne S., MacBeth C. (1994). Inversion for seismic anisotropy using genetic algorithms. *Geophys Prospect* 42(8), 953-974.
9. Inman J.R. (1975). Resistivity inversion with ridge regression. *Geophys,* 40, 788-817.
10. Kirkpatrick S., Gelatt C.D. Jr, Vecchi M.P. (1983). Optimization by simulated annealing. *Science,* 220, 671-680.
11. Koefoed O. (1970). A fast method for determining the layer distribution from the raised Kernal function in geoelectrical soundings. *Geophys Prospect*, 18, 564-570.
12. Levenberg K (1944) A method for the solution of certain non-linear problems in least-squares. Q App Math 2:164-168.
13. Macias C.C., Sen M.K., Stoffa P.L. (2000). Artificial neural networks for parameter estimation in geophysics. *Geophys Prospect* 48, 21–47.
14. Maiti S., Gupta G., Erram V.C., Tiwari R.K. (2012). Delineation of shallow resistivity structure around Malvan, Konkan region, Maharashtra by neural network inversion using vertical electrical sounding measurements. *Environl Earth Sci*. http: / / doi.org / 10.1007 / s12665-012-1779-8
15. Marquardt D.W. (1963). An algorithm for least-squares estimation of non-linear parameters. *J Soc Industr Appl Math*, 11, 431-441.
16. Meju M.A. (1994). Geophysical data analysis: Understanding Inverse problem Theory and Practise. Soc Explor Geophys Course Notes Series No.6 1st Edition SEG Publishers Tulsa Oklahoma ISBN, 1-56080-027-5 296p.
17. Menke W. (1984). Geophysical data analysis: discrete inverse theory. Academic Press, Inc, New York.
18. Morgan W.J. (1972). Deep Mantle convection plumes and plate motions. *Bull Am Assoc Pet Geol,* 56, 203–213.
19. Nyman D.C., Landisman M. (1977). VES Dipole-Dipole Filter Coefficients. *Geophys* 42(5), 1037-1044.
20. Parker R.L. (1994). Geophysical Inverse Theory. Princeton Univ. Press, Princeton, N. J.
21. Puranik S.C. (2009). Occurrence and quality characterization of groundwater in hard rock terrains of Karnataka. *J Geol Min Res* 1, 208–213.
22. Roy I.G. (1999). An efficient non-linear least-squares 1D inversion scheme for resistivity and IP sounding data. *Geophys Prospect*, 47, 527-550.

23. Rubinstein R.Y. (1981). Simulation and the Monte Carlo method. Wiley, New York, 278p.

24. Sarkar P.K., Soman G.R. (1986). Geology of the area around Katta Sindhudurg district based on aerospace data. *J Indian Soc Remote Sensing* 14(2), 43-51.

25. Song S.H., Lee J.Y., Park N. (2007). Use of vertical electrical soundings to delineate seawater intrusion in a coastal area of Byunsan, Korea. *Environ Geol*, 52, 1207-1219.

26. Tandale TD (1993) Coastal environ of maharashtra- evolution and human activities aided with satellite remote sensing. J Indian Soc Remote Sens. 21(2), 59-65.

27. Verma R.K., Rao M.K., Rao C.V. (1980). Resistivity investigations for ground water in metamorphic areas near Dhanbad, India. Ground Water, 18(1), 46-55.

28. World Health Organization (WHO) (1984). Guideline of drinking quality. Washington, World Health Organization 333-335.

29. Zohdy A.R. (1989). A new method for automatic interpretation of Schlumberger and Wenner Sounding curves. *Geophys,* 54, 245-253.